Ferroresonance in MV Voltage Transformers: Pragmatic experimental approach towards investigation of risk and mitigating strategy

W. Piasecki, M. Stosur, T. Kuczek, M. Kuniewski, R. Javora

***Abstract*-- Evaluation of risk of ferroresonance in voltage transformers is typically performed by transient simulations using non-linear models of instrument transformers. In the process of selection and optimization of mitigating and damping approach the experimental verification is always required at the final stage. Such experiments performed on full-scale devices are complex, costly and hazardous, as the ferroresonance in VTs is associated with a risk of a ground-fault.**

In the present paper an experimental set-up is presented, allowing one to perform studies of ferroresonance in a safe, low voltage environment. The set-up comprises a separating transformer providing an ungrounded 3-phase LV network supply. Ferroresonant conditions were investigated for variable network capacitance taking into account capacitance values scaling to the LV network level. Both in the simulations and in the experiments the ferroresonant oscillations were initiated by an intermittent single-phase earth-fault. Using the described set-up realistic values of the hazardous, ferroresonant capacitances in a real MV grid could be found, matching those obtained using simulations. Effectiveness of ferroresonance damping was also demonstrated and compared against simulations. The methodology presented in the paper has been demonstrated as an efficient way of evaluating the risk of ferroresonance and applicability of particular damping methods.

***Keywords*: Ferroresonance, Voltage Transformers.**

I. Introduction

Voltage transformers are transformers characterized by a special construction and their rated power is typically very low due to their metrological, rather than power supply function. Nominal primary currents in the voltage transformer (VT) winding are typically in the order of single mA at primary voltage ranging from several up to tens of kilovolts in MV networks, and hundreds of kV in HV networks.

Special construction of voltage transformers characterized by their relatively low power ratings makes them potentially very sensitive to the ferroresonance problem since large overcurrent in the primary windings may lead to the overheating and, in consequence, to the permanent equipment damage. Incidents of catastrophic failures of voltage transformers results in high costs as are constituted by the equipment replacement cost, electricity outage costs, and potential damage to the adjacent substation equipment. The reasons of the failure are often misunderstood and attributed to the manufacturing error. Thus, the replacement of the VTs does not solve the root cause and the event of fault may soon re-occur. It is not a rare case that after several consecutive replacements of equipment, the faulty VTs are investigated concluding that the root cause was related to ferroresonance. It is important to clearly state that the ferroresonance is not involving the VT alone, but it is a network phenomenon considering the VT and capacitance present in the network. Therefore, investigation of the potential ferroresonance phenomenon cannot be performed for the VT alone, without knowing particular network configuration and its parameters, mainly capacitances, which take active part in the ferroresonance phenomenon occurrence.

Ferroresonance is a non-linear resonance between the capacitance (linear element) and a non-linear inductance. Most of the inductive elements present in power network (transformers of various types and reactors) use magnetic cores. These devices are designed within the region in which the magnetizing curve of the core is close to linear. Except from transient situations, such as transformer energization, when temporary core saturation results in the inrush current, the inductances in the system are well defined. In system configurations, in which at least one terminal of the inductive device is connected to a node, whose potential is not fixed, but coupled to the system source through some capacitance, a resonant circuit is created. Since the inductance is non-linear, a special type of circuit is formed, which may, under special conditions, fall into the resonant interaction called ferroresonance. This phenomenon has been investigated for many years and there is a very broad literature in this area covering the theory, simulations and modelling techniques (e.g. [1,2,3]), identification and analysis of effects of ferroresonance (e.g. [4,5]), as well as mitigation [6-8]. Recently a very comprehensive CIGRE document [9] has been released providing high level, in-depth explanation of the phenomenon as well as gives an overview of the typical ferroresonant configurations, which could be found in practical electrical power networks.

W. Piasecki, T. Kuczek and M. Stosur are from ABB Corporate Research Center in Krakow, Poland (e-mail of corresponding author: wojciech.piasecki@pl.abb.com).

M. Kuniewski is from Department of Electrical and Electrical Power Engineering, AGH University of Science and Technology in Krakow, Poland (email: maciek@agh.edu.pl).

R. Javora is from ABB Department of MV Instrument Transformers & Sensors in Brno, Czech Republic (email: radek.javora@cz.abb.com)

Paper submitted to the International Conference on Power Systems Transients (IPST2017) in Seoul, Republic of Korea June 26-29, 2017

In MV networks ferroresonance most typically takes place in 3-phase ungrounded systems as a result of system disturbance, such as system start-up, intermittent earth-fault, or system re-configuration (e.g. connecting of a cable feeder at MV substation). In this case ferroresonance is possible in the normally energized system and has a form of zero-sequence oscillations. Detailed analysis of the problem of ferroresonance in MV ungrounded networks can be found e.g. in [8].

In the impedance-grounded system (grounding resistor or Petersen coil) the impedance of the grounding device is substantially dominating that of the VTs and therefore the ferroresonance involving the VTs is practically not possible. There has been neither simulation results no field failures reports in which this configuration resulted in ferroresonance involving VTs.

Despite the fact that the phenomenon has been known for many years and that numerous publications in this area exist, in fact no simple and reliable criteria can be formulated allowing one to assure the ferroresonant-free operation of a particular VT type on the basis of design data. Therefore the verification of the ferroresonant-free operation has to be performed using case-by-case approach on the basis of very accurate model of the VT precisely reflecting its non-linear characteristics, core losses, winding resistances, leakage inductances and capacitances.

The ultimate verification is an experiment which validates the simulation model. The experimental verification is not necessarily required for all conditions for which the ferroresonant-free operation must be verified. Once the model is validated in both ferroresonant and non-ferroresonant conditions indicating agreement between the simulation and experiment, its behaviour can be extrapolated to cases, for which the experimental validation cannot be performed due to practical or economic reasons. Experimental verification of the ferroresonance simulations requires use of physical units as these operating in the MV networks.

Performing full-scale experiments in a realistic set-up comprising a MV network environment is costly and hazardous, due to potential realistic consequences of primary winding short-circuit. An alternative described in the present article is based on the scaling principle. The physical VT units used in the present study comprise the magnetic circuits (cores) and secondary windings of a real MV VTs used in production, their primary windings however, are sized so that experiments can be performed at low voltage conditions. The interpretation of the results and their extrapolation to realistic MV voltage levels can be done, having in mind that the resonant phenomena investigated, involve network capacitance. This capacitance must be scaled according to the transformation ratio between the voltage level used in the experimental set-up and the realistic network level.

II. Voltage transformers and the experimental set-up

A. Voltage transformers

The physical VT units, for which the simulations and experiments were performed were specially designed and fabricated, based on the real MV production units. The magnetic cores and secondary windings are standard production elements. The number of turns in primary windings were calculated so that the VT primary nominal voltage was 173 V/√3, for which the core flux density was 0.9 T. From the equivalent circuit point of view adjustment of the primary side voltage to the realistic MV level can be done by adding an ideal transformer to the primary of the present VT. Since an ideal transformer converts the impedance with a square of the transformation ratio, the resonant phenomena investigated in the present LV set-up are identical to those in the MV network for capacitance values scaled with the square of the voltage ratio. This is explained schematically in Fig. 1.

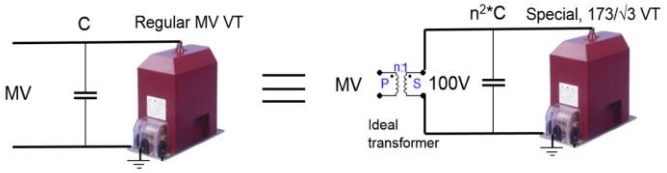

Fig. 1. Explanation of the scaling principle implemented in the present study; left: MV network comprising a regular MV unit and the network capacitance *C*; right: experimental LV unit and ideal transformer

The primary windings of the VTs used in the present studies were rated at 173 V/√3, which corresponds to 100 V of the line-to ground (L-G) voltage. Table 1 shows exemplary values of the L-G capacitances in the 173 V network and the corresponding capacitance values in a 20 kV networks. Selected values reflect realistic L-G values in MV networks, for which the ferroresonance risk was studied. The values marked in yellow are those covered in the experimental studies described later.

TABLE I
SELECTED L-G VALUES IN THE 173 V/√3 NETWORK AND CORRESPONDING CAPACITANCES IN THE REALISTIC 20 KV/√3 NETWORK

Network type	Equivalent capacitances								
173 V / √3	130 µF	260 µF	390 µF	540 µF	800 µF	930 µF	1170 µF	1600 µF	1950 µF
20 kV / √3	10 nF	20 nF	30 nF	40 nF	60 nF	70 nF	90 nF	120 nF	150 nF

The experimental VT comprised 2 secondary windings: 100/√3 (marked a-n), and 100/3 (marked da-dn) respectively. The electrical parameters of the VTs (magnetizing characteristic, winding resistances and leakage inductances) were measured and used for building of an equivalent VT model described in the next section.

B. Experimental set-up

The LV experimental laboratory set-up used for investigation of the ferroresonance in VTs and effectiveness of damping is presented in Fig. 2. The set-up is supplied through a 3-phase separating transformer with a star-connected secondary winding with isolated neutral point and a three phase autotransformer (Fig. 3). This forms a local, 3-phase isolated system with the voltage level U_n = 173 V/√3 (L-G voltage equal to 100 V). This voltage is adjustable from 0% to 130% of U_n. Phase-to-ground network capacitance can be selected within the range marked in yellow in Table I. The capacitance could be

adjusted from 130 µF up to 930 µF, which corresponds to C = 5÷75 nF in the 20 kV network.

Ferroresonance can be initiated by an intermittent earth-fault in one of the phases. L-G voltages, neutral point voltage as well as primary currents in the VT's can be monitored using a dedicated LabView software, also used to control the experiment sequence and values of the network capacitances.

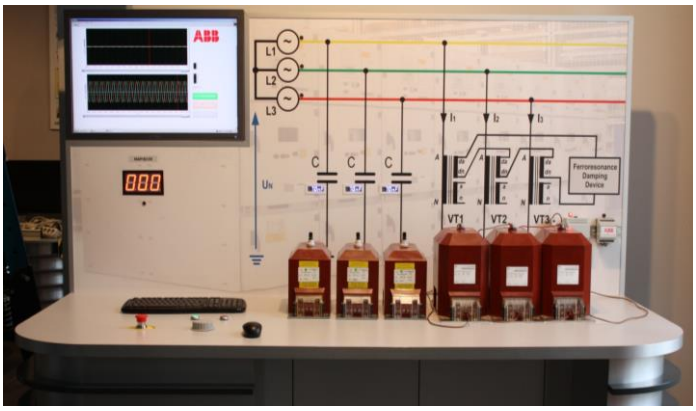

Fig. 2. Laboratory set-up – overview

The circuit diagram of laboratory setup is presented in Fig. 3 (corresponding to Fig. 2). Technical parameters of the FerroLab set-up is presented in Table II.

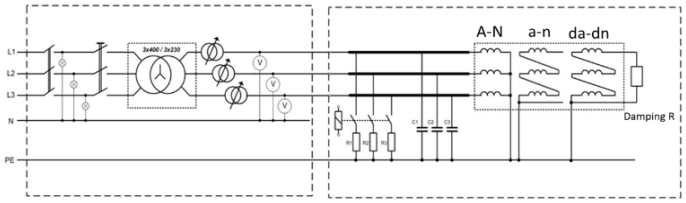

Fig. 3. Diagram of the network model used in ferroresonance investigation

TABLE II
DESCRIPTION OF THE LABORATORY SETUP FOR FERRORESONANCE EXPERIMENTS

Component	Parameters	Value
Supply grid	Nominal L-G voltage	U_N = 100 V
	Capacitance range	C_n = 130 µF to C_n = 930 µF
Autotransformer	Nominal power	S_N = 8 kVA
	Output voltage regulation range	0÷130% U_N
Voltage transformer	Primary voltage (A-N winding)	173V/√3 (100V line-to-ground)
	Secondary voltage (a-n)	100V/√3
	Secondary voltage (da-dn)	100V/3
	Nominal power	S_{VT} = 200 VA
	Class	0.5
	Thermal voltage factor k_t	1.9 U_N / 8h

III. FERRORESONANCE SIMULATIONS

In order to identify the ferroresonant conditions (network capacitance and network voltage) as well as damping efficiency using a resistive burden connected to open-delta arranged secondary windings of VT's, transient simulations were performed using EMTP-ATP software.

A. Voltage transformer model

The model of the voltage transformer was based on manufacturer's data as well as measured electrical quantities. The model reflects VT's magnetization characteristic, leakage inductance and resistances of windings, iron losses. The mutual coupling between primary and secondary coils was determined analytically knowing the geometries of the coils and the numbers of turns and verified in the measurements. Including the mutual coupling between the coils was applied to the VT model allowed to achieve higher level of convergence between measurement and simulation results as model of the VT was also realistically representing the air-coupling between the physical VT windings which is relevant to the analysis of damping using a burden connected to the secondaries. The complete simulation model of the VT used for simulations is shown in Fig. 4.

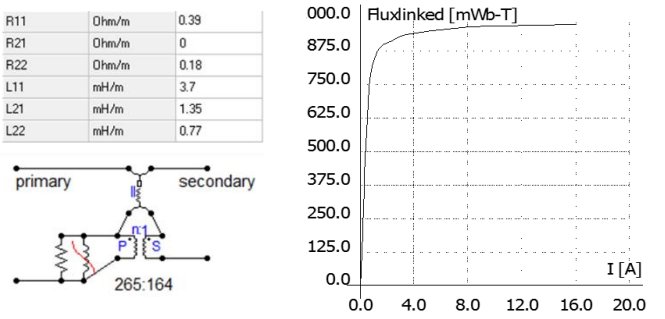

Fig. 4. Left: complete simulation model of VT comprising leakage inductances of primary (A-N) and secondary (a-n) coils represented by lumped *RL* line; air-coupling between primary and secondary coils included; right: magnetizing characteristic of the core

In the EMTP-ATP, mutual inductance was represented by means of lumped RL line, mutually coupled 2-phase component (named *LINERL_2*). It allows to provide the model with primary, secondary and mutual inductances and resistances (see Fig. 4). The resistance representing iron losses was calculated on the basis on measured iron losses of a production sample of a VT. The magnetizing characteristic was based on measured voltage-current curve (peak-to-peak), which was recalculated then to flux-current characteristic. It was corrected taking into account the values of leakage inductances and resistances of the windings. These were calculated based on the measurements and detailed design data of the VT, hence magnetic flux path, number of turns and cross sectional area of the iron core. Final characteristic that was implemented into the EMTP-ATP software is presented in Fig. 4.

B. Network model

In the simulations, a three-phase ungrounded network (173 V/√3) was modelled as three single-phase voltage sources. Phase-to-ground network capacitances were represented by lumped capacitors. The initiation of ferroresonance was done by a 500 ms ground-fault in one of the phases. Simulations were performed for various values of network capacitance and network voltage level, reflecting realistic situation of temporary

overvoltages. The ferroresonance damping by open-delta connected resistive burden was included.

C. Simulation results

In the present section results of simulation-based identification of potentially ferroresonant combinations of network capacitance and actual network voltage are presented. The criteria used in verification of the type of the system response is based on the analysis of the simulated voltage and current waveforms as indicated in Fig. 5.

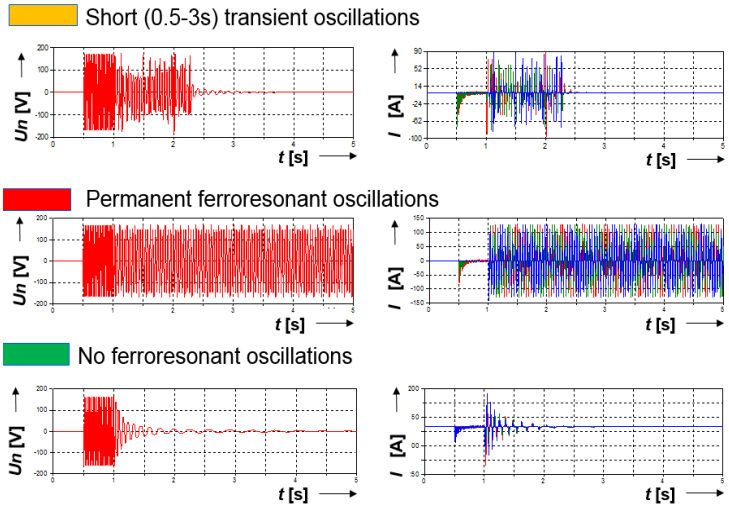

Fig. 5. Criteria of determining the ferroresonant vs non-ferroresonant response; U_n: neutral point voltage. I: primary VT currents (I_1, I_2, I_3)

Based on the criteria defined in Fig. 5 the results obtained for the resistive damping element connected to the *a-n* winding are summarized in Fig. 6. As a reference identification of ferroresonant regions with no damping was performed indicating that at the nominal voltage level ferroresonance is potentially possible at L-G network capacitance values of 540÷2600 µF, which corresponds to 40÷200 nF in a MV (20 kV/√3) ungrounded network without any damping. As the resistive damping is introduced, ferroresonance is practically eliminated below 47 Ω.

No damping

U	130 uF	260 uF	390 uF	540 uF	800 uF	930 uF	1170 uF	1600 uF	1950 uF	2600 uF	3250 uF	3900 uF
100%												
110%												
120%												
130%												

47 Ohm on *a-n* (100/V3)

U	130 uF	260 uF	390 uF	540 uF	800 uF	930 uF	1170 uF	1600 uF	1950 uF	2600 uF	3250 uF	3900 uF
100%												
110%												
120%												
130%												

27 Ohm on *a-n* (100/V3)

U	130 uF	260 uF	390 uF	540 uF	800 uF	930 uF	1170 uF	1600 uF	1950 uF	2600 uF	3250 uF	3900 uF
100%												
110%												
120%												
130%												

Fig. 6. Damping of ferroresonance by resistor connected to open-delta *a-n* windings

The situation changes, when the resistive damping is connected to the *da-dn* windings (Fig. 7). In this case much lower resistance value must be used. In this case resistance values well below 20 Ω are required. This results out of the fact that the voltage of the *da-dn* open-delta winding is lower than the voltage of the a-n open-delta windings by a factor of √3. As the power dissipated in the damping resistor equals to U^2/R, damping effect of the 27 Ω resistor connected to the *a-n* winding is similar to a resistor of 27 Ω/3 = 9 Ω. In the same way, the damping effect of the 47 Ω resistor connected to the *a-n* winding is similar to a resistor of 47 Ω/3 = 16 Ω. The value of 16 Ω, da-dn open-delta connected resistor can be regarded as the maximum resistance value, eliminating the risk of ferroresonance in this particular case. This value must then be confronted against the thermal limits of the VT. Under the prolonged earth-fault condition, the power dissipated in the damping resistor is $(3\times U_{\text{da-dn}})^2/R$, which in case of connecting the 16 Ω resistor results in $(100\ \text{V})^2/16\ \Omega = 625$ W at the nominal network voltage.

47 Ohm on *da-dn* (100/3)

U	130 uF	260 uF	390 uF	540 uF	800 uF	930 uF	1170 uF	1600 uF	1950 uF	2600 uF	3250 uF	3900 uF
100%												
110%												
120%												
130%												

27 Ohm on *da-dn* (100/3)

U	130 uF	260 uF	390 uF	540 uF	800 uF	930 uF	1170 uF	1600 uF	1950 uF	2600 uF	3250 uF	3900 uF
100%												
110%												
120%												
130%												

20 Ohm on *da-dn* (100/3)

U	130 uF	260 uF	390 uF	540 uF	800 uF	930 uF	1170 uF	1600 uF	1950 uF	2600 uF	3250 uF	3900 uF
100%												
110%												
120%												
130%												

10 Ohm on *da-dn* (100/3)

U	130 uF	260 uF	390 uF	540 uF	800 uF	930 uF	1170 uF	1600 uF	1950 uF	2600 uF	3250 uF	3900 uF
100%												
110%												
120%												
130%												

Fig. 7. Damping of ferroresonance by resistor connected to open-delta *da-dn* windings

IV. Experimental Results

Experimental studies in the set-up described in section II-B were performed in order to verify the results of the simulations described in the previous section. Due to practical limitations of the set-up the experiments could be performed for L-G network capacitances ranging from 130 µF to 930 µF, which corresponds to 10÷70 nF in the 20 kV network (see Table 1).

Similarly to the simulations, ferroresonance was initiated by a 500 ms intermittent single-phase earth-fault. In each case 10 shots were performed and the test was regarded positive (ferroresonant initiated) if at least one case of permanent ferroresonance was initiated. The definition of ferroresonant, non-ferroresonant, or transient response was based on the same criterion as in the case of simulations. Exemplary experimental waveforms are shown in Fig. 8.

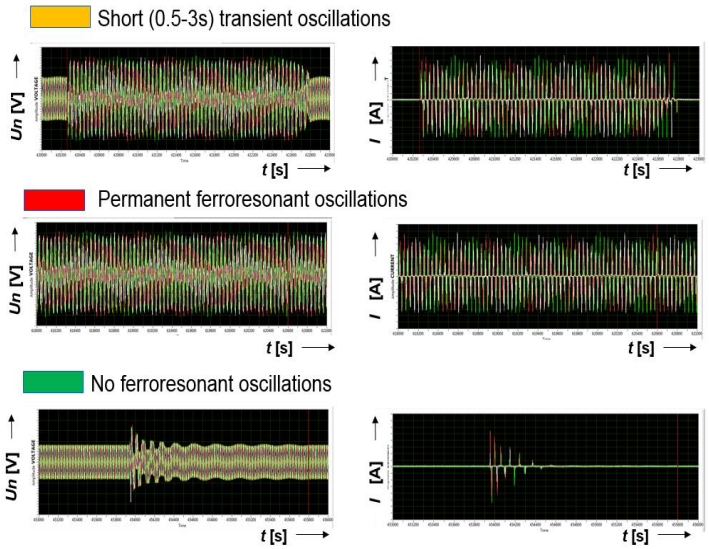

Fig. 8. Examples of recorded voltage and current waveforms indication the types of transient response to the intermittent earth-fault. Criteria of determining the ferroresonant vs non-ferroresonant response; U_n: neutral point voltage. I: primary VT currents (I_1, I_2, I_3)

The experimental results are summarized in Fig. 9. Due to the practical limitation of the present experimental set-up the experiments were performed for capacitance values up to 930 µF (corresponding to 70 nF of L-G capacitance in 20 kV network), which covered the lower range of the capacitances used in the simulations.

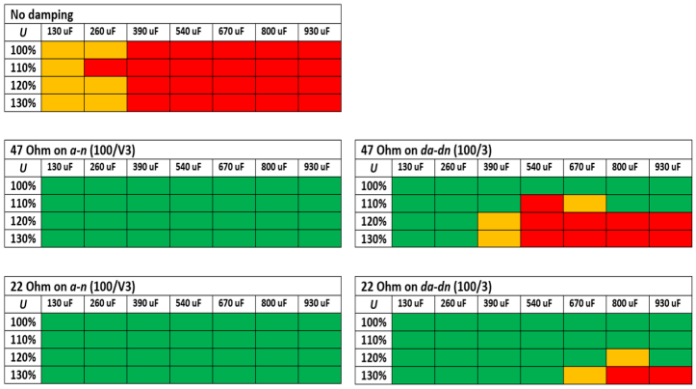

Fig. 9. Experimental studies of ferroresonance; left: no damping and resistive damping by resistor connected to open-delta *a-n* windings; right: damping of ferroresonance by resistor connected to open-delta *da-dn* windings

The results indicate that the ferroresonant capacitance lower limit matches very closely ones that were found in simulations. In the experiments with no damping permanent oscillations may even be initiated at capacitance slightly lower than simulated. The upper limit was not found due to experimental limitations. Damping with open-delta connected a-n was already efficient with a 47 Ω resistor, while in the case of da-dn windings cases of ferroresonance were recorded with 22 Ω resistor, at network voltage exceeding 120% U_n. This indicates that in experiments slightly larger resistor values were sufficient to eliminate ferroresonance and, hence simulation results provide some additional safety margin. This may be an effect of the assumed ideal model of the network neglecting the network impedance, so that the worst case scenario is considered. The sensitivity of the ferroresonance to this parameter can be demonstrated by including a small resistors, representing the source impedance. As an example, 0.1 Ω source impedance was included in the circuit and simulations were repeated for the 47 Ω resistor connected to the a-n windings, at L-G capacitance of 930 µF, at 120% of U_n voltage. In this specific case the simulations of the worst-case scenario indicated a ferroresonant response, while the experiments indicated already a non-ferroresonant response.

The qualitative difference confirms the statement that the phenomenon analysed is very sensitive to small changes in the system and devices parameters. Nevertheless the agreement between the simulations and experiment is sufficient for evaluating the damping efficiency and to extrapolate the studies to cases not covered by the experiment.

V. SUMMARY AND CONCLUSIONS

Special construction of voltage transformers characterized by their relatively low power ratings makes them potentially very sensitive to the ferroresonance problem since large overcurrent in the primary windings may lead to the overheating and, in consequence, to the catastrophic equipment damage. Ferroresonance analysis of specific type of VT has to be performed using case-by-case approach on the basis of very accurate model of the VT precisely reflecting its non-linear characteristics, core losses, winding resistances, leakage inductances and capacitances. The ultimate verification of ferroresonance-free operation and effectiveness of the damping method is experiment using physical VT units, validating the simulation model. Performing full-scale experiments in a realistic set-up comprising a MV network environment is costly and hazardous, and thus an alternative approach based on the scaling principle has been proposed and validated. It has been demonstrated that the physical VT comprising the magnetic cores and secondary windings of a real MV VTs may be tested at low voltage conditions. The interpretation of the results and their extrapolation to realistic MV voltage levels can be done.

VI. REFERENCES

[1] M.R, Irvani et al., "Modeling and analysis guidelines for slow transients — Part III: The study of ferroresonance", *IEEE Trans. Power Delivery*, vol. 15, no 1, pp. 255-265, 2000

[2] A. Ben-Tal, V. Kirk, G. Wake, "Banded chaos in power systems", *IEEE Trans. Power Delivery*, vol. 16, no 1, pp. 105-110, 2001

[3] Jacobson D.A.N., et al., "Stability domain calculations of period-1 ferroresonance in a nonlinear resonant circuit", *IEEE Trans. Power Delivery*, vol. 17, no 3, pp. 865-871, 2002

[4] T.A. Short, J.J. Burke, R.T. Mancao, "Application of MOVs in the distribution environment", *IEEE Trans. Power Delivery*, vol. 9, no 1, pp. 293-305, 1994

[5] R.A. Walling et al., "Performance of metal-oxide arresters exposed to ferroresonance in padmount transformers", *IEEE Trans. Power Delivery*, vol. 9, no 2, pp. 788-795, 1994

[6] M. Graovac et al., "Fast ferroresonance suppression of coupling capacitor voltage transformers", *IEEE Trans. Power Delivery*, vol. 18, no 1, pp. 158-163, 2003

[7] W. Piasecki, M. Florkowski, M. Fulczyk, P. Mahonen, M. Luto, W. Nowak, "Ferroresonance Involving Voltage Transformers in Medium Voltage Networks", *XIVth Inter. Symp. on the High Voltage Engineering*, Tsinghua University Beijing, F-19, 2005

[8] W. Piasecki, M. Florkowski, M. Fulczyk, P. Mahonen, W. Nowak, "Mitigating Ferroresonance in Voltage Transformers in Ungrounded MV Networks", *IEEE Trans. Power Delivery*, vol. 22, no 4, pp. 2362-2369, 2007

[9] CIGRE Technical Report 569, "*Resonance and Ferroresonance in Power Networks*", 2014